Chemical Geology 412 (2015) 82–91

Contents lists available at ScienceDirect

Chemical Geology

journal homepage: www.elsevier.com/locate/chemgeo

A refined dissolution method for rare earth element studies of bulk carbonate rocks

Kan Zhang, Xiang-Kun Zhu *, Bin Yan

Laboratory of Isotope Geology, MLR, State Key Laboratory of Continental Dynamics, Institute of Geology, Chinese Academy of Geological Sciences, Beijing 100037, China

ARTICLE INFO

Article history:
Received 20 May 2015
Received in revised form 21 July 2015
Accepted 22 July 2015
Available online 26 July 2015

Keywords:
Rare earth elements
Bulk carbonate rock
Stepwise dissolution
Diagenetic alteration
Non-carbonate contamination

ABSTRACT

Extraction of primary geochemical signals from bulk carbonate rocks is a key task in palaeoenvironmental studies. REE behaviour is investigated during stepwise dissolution of carbonate rocks. The experiment is designed to achieve total carbonate dissolution in ten steps, aiming for approximately 10% of the total carbonate to be dissolved in each step using acetic acid. An additional eleventh step using excess acid completed each experiment. Results show that calcite is preferentially dissolved before dolomite though no significant effect on the REE pattern of the rock is observed. Secondary carbonate phases and adsorbates are likely to be dissolved at the beginning of the dissolution process but this does not increase REE concentration though the REE pattern may be altered e.g. lessening of negative Ce anomaly, altering of Eu anomaly, Y/Ho ratio and relative fractionation between LREE and HREE. Non-carbonate minerals e.g. terrestrial particulate matter, Fe–Mn oxyhydroxides and phosphates, are likely to be dissolved towards the end of the total dissolution, especially in the final excess acid step. This should increase REE concentrations and alter REE distribution patterns greatly. In contrast, solutions from intermediate steps are less contaminated. Further, compared with using 10% v/v acetic acid, the solutions obtained using 5%v/v acid return more pristine REE information from the carbonate.

A proposed method for REE studies of bulk carbonate rocks requires an initial dissolution of 30%–40% followed by the sampling dissolution of 30%–40% of total carbonate using 5%v/v acetic acid to produce REE information considered to best represent that of the carbonate source water. Following these steps 20%–30% of the carbonate should remain undissolved, thus minimising contamination from non-carbonate minerals.

1. Introduction

The rare earth element (REE, including yttrium) geochemistry of authigenic carbonates has shown itself to be an important tool for studying the water from which they precipitated (Webb and Kamber, 2000; Nothdurft et al., 2004; Shields and Webb, 2004; Ge et al., 2010; Delpomdor et al., 2013). Similar ionic radii and the predominance of trivalent valence states make the lanthanide series (including Y) act as a coherent group during geological and geochemical processes. However, small but systematic differences in the properties of REE make it possible to use them to constrain depositional environments of ancient carbonate rocks (Cantrell and Byrne, 1987; Lee and Byrne, 1993; Bolhar et al., 2004; Nothdurft et al., 2004; Bolhar and Van Kranendonk, 2007; Pourret et al., 2007; Frimmel, 2009; Rongemaille et al., 2011). For example, the Ce anomaly can be used as a redox tracer. Redox-sensitive Ce exists in either trivalent or tetravalent form, and soluble Ce^{3+} can be oxidized to highly insoluble Ce^{4+} in oxygenated water. Thus a negative Ce anomaly exists in oxygenated water and the carbonate rocks precipitated from it; correspondingly, a positive Ce anomaly exists in Fe–Mn sediments where the tetravalent Ce ion is prone to be adsorbed (Elderfield et al., 1981; Elderfield and Sholkovitz, 1987; Bau et al., 1996; Slack et al., 2007; Birgel et al., 2011; Ling et al., 2013; Loope et al., 2013). Eu^{3+} can be reduced to Eu^{2+} under extremely reducing conditions. However, a Eu anomaly in seawater may not reflect the redox state of water, but is generally regarded as an indicator of hydrothermal input (Derry and Jacobsen, 1990; Danielson et al., 1992; Wheat et al., 2002; Bolhar and Van Kranendonk, 2007; Frimmel, 2009; Wang et al., 2014). The Y/Ho ratio can serve as a monitor for differentiating between different water types (Nozaki et al., 1997; Wang et al., 2014). Seawater has a higher Y/Ho ratio than freshwater, and the elevated Y/Ho ratio results from Ho being scavenged two times faster than Y from the surface ocean to the deep ocean because of different surface complexing behaviour (Nozaki et al., 1997). Generally, the PAAS-normalized REE distribution patterns of typical marine carbonates are similar to modern seawater which is characterized by an enrichment of HREE, a positive La anomaly (~2.62 in average), negative Ce anomaly (in oxygenated condition), subtle positive Gd anomaly and a superchondritic Y/Ho ratio (44–74) (Bau et al., 1996; Zhang and Nozaki, 1996; Bolhar et al., 2004; Shields and Webb, 2004; Lawrence et al., 2006). By contrast, freshwater carbonates display slight LREE depletion or enrichment, or MREE enrichment, no distinct element anomalies, and

* Corresponding author.
E-mail address: xiangkun@cags.ac.cn (X.-K. Zhu).

http://dx.doi.org/10.1016/j.chemgeo.2015.07.027
0009-2541/

near-chondritic Y/Ho ratios (Sholkovitz et al., 1999; Lawrence et al., 2006; García et al., 2007).

When using REE for palaeoenvironmental studies, it is crucial to ensure that the information extracted from bulk carbonate rocks is not affected by diagenetic alteration or contaminated by non-carbonate materials. Although diagenetic fluids are generally considered to have little effect on the primitive REE features in carbonate rocks due to their low REE concentrations (Banner et al., 1988; Sholkovitz et al., 1989; Banner and Hanson, 1990; Webb and Kamber, 2000; Lin et al., 2011), this does not mean their influences can be entirely ignored (Shields and Stille, 2001; Bolhar and Van Kranendonk, 2007; Ling et al., 2013). Moreover, possible contamination from non-carbonate minerals, such as terrestrial particulate matter, Fe–Mn oxyhydroxides and phosphates, can never be dismissed (Elderfield, 1986; Elderfield et al., 1990; Bau et al., 1996; Nothdurft et al., 2004). To deal with these potential problems, various partial dissolution methods have been proposed. For examples, in the study of Nothdurft et al. (2004), the carbonates for REE determination were obtained through dissolving samples in ultra-pure 1 M acetic acid; in the study of Zhao et al. (2009), samples were dissolved in 0.5 M acetic acid at room temperature for 4 h; in the study of Rongemaille et al. (2011), the use of 5%v/v acetic acid at room temperature with duration of 24 h is recommended. However, no systematic investigation on the REE behaviour during dissolution of carbonate rocks has been conducted in previous studies. This leaves some uncertainty over the accuracy of the proposed dissolution methods.

Detailed stepwise dissolution experiments, for example in the study of strontium isotope stratigraphy (SIS) by Bailey et al. (2000), may well separate REE signals from different components in bulk carbonate rocks, including different carbonate phases and non-carbonate materials. Thus the genuine signature reflecting the water-column from which the carbonates precipitated may be recovered or obscured depending on the dissolution process. This paper reports the results of such experiments, and accordingly proposes a refined dissolution method for the REE study of bulk carbonate rocks.

2. Materials and methods

2.1. Experimental design

In the stepwise dissolution experiments, about 10% of total sample carbonate is designed to be dissolved in each step, thus requiring ten steps. This is followed by an eleventh step during which sample residue is treated with excess dilute acetic acid. Previous studies indicate that dilute acetic acid can minimise the contamination from non-carbonate minerals while dissolving calcite and dolomite (Bailey et al., 2000; Zhao et al., 2009; Li et al., 2011; Rongemaille et al., 2011). To investigate the effect of acid strength, 5%v/v (0.86 M) and 10%v/v (1.73 M) acetic acid are used for comparison. Samples of different types of carbonate rocks are selected for investigation.

2.2. Samples

A limestone, a calcareous dolostone, a siliceous dolostone and a pure dolostone were prepared for the stepwise dissolution experiments.

Sample L refers to a limestone collected from the third Member of Mesoproterozoic Gaoyuzhuang Formation in Jixian Section, North China. It contains 46.38% CaO and 5.56% MgO, and the contents of SiO_2, Al_2O_3 and TFe_2O_3 are 6.13%, 0.24% and 0.14%, respectively.

Sample CD refers to a calcareous dolostone collected from Neoproterozoic Doushantuo cap carbonate in Tianjiayuanzi Section, South China. It contains 31.55% CaO and 13.33% MgO, and the contents of SiO_2, Al_2O_3 and TFe_2O_3 are 10.21%, 2.56% and 1.40%, respectively.

Sample SD is a siliceous dolostone collected from Neoproterozoic Doushantuo cap carbonate in Jiulongwan Section, South China. It contains 15.84% CaO and 10.57% MgO, and the contents of SiO_2, Al_2O_3 and TFe_2O_3 are 39.92%, 3.91% and 2.75%, respectively.

Sample D is the powdered dolostone standard SRM 88b purchased from the National Institute of Standards and Technology (NIST), U.S. It contains 29.95% CaO and 21.03% MgO, and the contents of SiO_2, Al_2O_3 and TFe_2O_3 are 1.13%, 0.336% and 0.277%, respectively.

Concentrations of Ca, Mg, Si, Al, and Fe of the first three samples were analysed with an X-ray fluorescence spectrometer in the National Research Center for Geoanalysis, China, while those of Sample D were obtained from the NIST material database.

For Sample L, the powders used for experiments were obtained by micro-drilling on a fresh surface of a rock slab; whereas Samples CD and SD were first broken into small pieces, and clean fragments were then selected and pulverized in an agate mortar. For both physical extraction methods, efforts were made to avoid veins, later-stage cements, etc.

2.3. Experimental procedure

All experiments were carried out in a class 100 ultra-clean laboratory in the Laboratory of Isotope Geology, Institute of Geology, Chinese Academy of Geological Sciences. Acids used in the study were purified using DST-1000 device from American Savillex company, and 18.2 MΩ-cm ultrapure water was prepared by PURELAB® ultra water system from British Elga company. All containers and pipette tips used were cleaned thoroughly following strict procedures.

Sample powders (~0.6 g) were weighed in 50 ml polypropylene centrifuge tubes, and two sets of materials were prepared for dissolution using 5%v/v and 10%v/v acetic acid respectively. The volumes of dilute acetic acid used in each steps were calculated to dissolve 10% of carbonate, the content in each sample being estimated from its total CaO and MgO. The calculated volume of acetic acid was added into samples in their centrifuge tubes, then the tubes were sonicated intermittently in an ultrasonic bath. The reaction time was fixed at 24 h, ensuring a complete reaction (no more bubble generation). The leachates were obtained by centrifuging, while the residue was rinsed three times using ultrapure water. The water was then added to the previous supernatant. This partial dissolution procedure was repeated another 9 times, and a total of 10 leachates were obtained from each tube. Finally, excess 5%v/v or 10%v/v acetic acid (about 5 times of the previous volume) was added into each tube to get the eleventh leachate. After the entire stepwise extraction, all the leachates were converted to nitric acid medium, and an aliquot of each leachate was then taken for elemental analysis.

The elemental analysis was carried out at the State Key Laboratory for Mineral Deposits Research, Nanjing University. There, the dried aliquots were dissolved in 5 ml 3% HNO_3, and 100 μl Rh (200 ppb) was added in each sample as an internal standard for correcting matrix effects and instrument drift. The trace elements were determined using a Finnigan MAT ELEMENT 2 ICP-MS, and the major elements were measured by ICP-AES of JY3S, with analytical precisions better than 5% and 2% respectively. Some samples were diluted 20-fold again for Ca or Mg determination.

3. Results

The data are not included in this publication but are available in the online Appendix, their main features are described in the following text.

3.1. Ca and Mg

Variations in the amount of Ca + Mg released during the stepwise dissolution process are shown in Fig. 1a. Among the first nine or ten steps, the Ca + Mg released in each step is approximately 10% of the total Ca + Mg in each sample, and becomes much lower in step 11. For Sample L, the amount declines in step 10, especially for the series treated with 10%v/v acetic acid. These results indicate that the carbonate content in the samples has been almost totally consumed during the first ten steps as expected. Variations in the Mg/Ca molar ratio

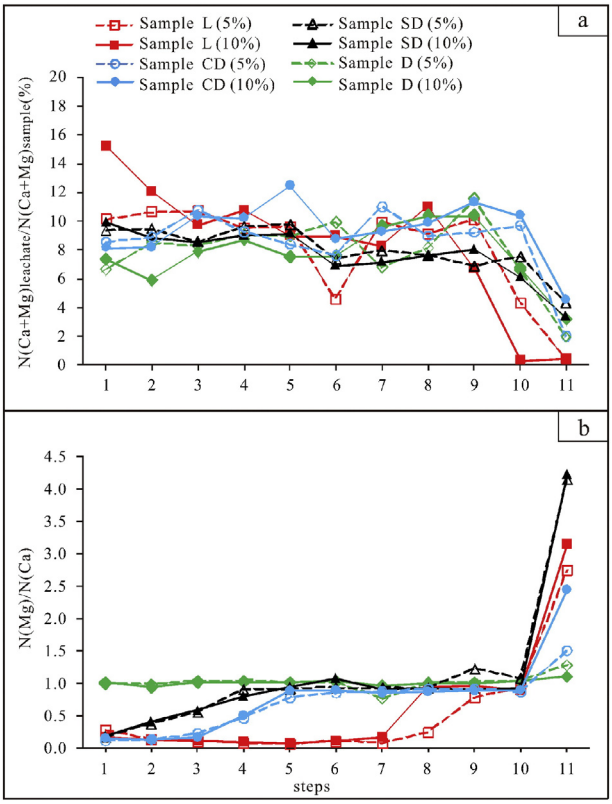

Fig. 1. Variations in the number of moles of Ca + Mg (a) and molar ratio of Mg/Ca (b) during the stepwise dissolution process of carbonate samples.

during the stepwise dissolution process are shown in Fig. 1b. For Sample L, a limestone, the Mg/Ca molar ratios are low in the first eight steps of the first series (treated with 5%v/v acetic acid) and the first seven steps of the second series (treated with 10%v/v acetic acid), at about 0.1 on average. The ratios increase to near unity in the following two or three steps, and become much higher than 1 in step 11 for both series (2.7 and 3.1 respectively). For Sample CD, a calcareous dolostone, the Mg/Ca molar ratios are low in the first three steps, ~0.2 on average. The ratios increase to near unity from the fifth to tenth step, and become higher than 1 in step 11 for both series (1.5 and 2.4 respectively). For Sample SD, a siliceous dolostone, the Mg/Ca molar ratios increase from ~0.2 in step 1, to ~1 in step 5, then remaining steady until step 10; the ratios reaching ~4 in step 11 for both series. For Sample D, a dolostone, the Mg/Ca molar ratios are fairly stable at ~1 during the first ten steps for both series, becoming slightly higher in step 11.

3.2. Rare earth elements

The rare earth element content of each leachate is converted into the equivalent concentration in the carbonate component consumed in each dissolution step. The weight of ($CaCO_3$ + $MgCO_3$) consumed in each step is estimated by assuming that all the Ca and Mg in the leachates result from dissolution of carbonate. It is necessary to point out that, for step 11, the much lower Ca and Mg contents may lead to extremely high concentrations of rare earth elements and other diagnostic elements (see Section 3.3), however, this just highlights the dissolution of non-carbonate minerals and their effects on primitive REE of carbonate rocks reflecting deposition environment (see Section 4.3), but would not influence the evaluation result in Section 4.4. The rare earth elements are finally normalized to Post-Archean Australian Shale (PAAS) (Taylor and McLennan, 1985) (Fig. 2). In order to guard against the appearance of anomalous REE patterns, the near neighbours used in the anomaly calculation must not show any anomalous behaviour themselves. In our analysis, anomalies for La, Ce, and Eu are obtained by the following formulae: $La/La^* = La_n/\{Pr_n \times (Pr_n/Nd_n)^2\}$, $Ce/Ce^* = Ce_n/\{Pr_n \times (Pr_n/Nd_n)\}$, $Eu/Eu^* = Eu_n/\{(Sm_n^2 \times Tb_n)^{1/3}\}$ (Lawrence et al., 2006).

As can be seen from Fig. 2, REE concentrations and/or distribution patterns obtained from different leachates of the same sample can be rather different. Particularly for Samples L, CD and SD, the first and last few steps, notably step 1 and step 11, generally exhibit REE characteristics more variable than intermediate ones. Moreover, there are some REE differences between the two series (dissolved with 5%v/v and 10%v/v acetic acid) of one sample.

For Sample L, the REE concentrations are low in the first eight steps of the series treated with 5%v/v acetic acid and the first seven steps of the series treated with 10%v/v acetic acid, then obviously increase in the following three or four steps. The REE distribution patterns are mostly characterized by (1) slight LREE depletion; (2) positive La anomalies with $[La/La^*]_{PAAS}$ from 1.0 to 4.3; (3) nearly no Eu anomalies; and (4) super-chondritic Y/Ho ratios of 35.2–72.8. As for Ce anomalies, only step 4 to step 7 in the series treated with 5%v/v acetic acid exhibit obvious negative Ce anomalies with $[Ce/Ce^*]_{PAAS}$ ~ 0.5 on average; other steps exhibit nearly no Ce anomalies with $[Ce/Ce^*]_{PAAS}$ from 0.9 to 1.2.

For Sample CD, step 11 for both series exhibit abnormally high REE concentrations. Among the first ten steps, the REE concentrations increase in the latter stages, especially for the second series. Except for steps 1 &11, the REE distribution patterns of the other steps are similar and characterized by (1) LREE enrichment; (2) positive La anomalies with $[La/La^*]_{PAAS}$ from 1.5 to 2.4; (3) nearly no Ce anomalies with $[Ce/Ce^*]_{PAAS}$ from 0.9 to 1.2; (4) subtle positive Eu anomalies with $[Eu/Eu^*]_{PAAS}$ from 1.6 to 2.4; and (5) near-chondritic Y/Ho ratios from 26.0 to 41.7 (~34 on average). Step 1 for both series exhibit nearly no fractionation between LREE and HREE, and higher Y/Ho ratios of about 46. Step 11 for both series show almost no La anomalies, and the lowest Y/Ho ratios of 15.8 and 18.8 respectively. Meanwhile, step 11 for the first series displays a slight positive Ce anomaly with $[Ce/Ce^*]_{PAAS}$ ~ 1.5.

For Sample SD, step 11 for both series also exhibit abnormally high REE concentrations. In the first series, the REE concentrations are low for the first nine steps, becoming significantly higher in step 10. The REE concentrations in the first ten steps of the second series are on average higher relative to those of the first series. Similarly to the results from Sample CD, the REE distribution patterns of other steps excepting step 1 and step 11 are characterized by (1) LREE enrichment; (2) positive La anomalies with $[La/La^*]_{PAAS}$ from 1.6 to 3.2; (3) nearly no Ce anomalies with $[Ce/Ce^*]_{PAAS}$ from 0.8 to 1.2; (4) subtle positive Eu anomalies with $[Eu/Eu^*]_{PAAS}$ from 1.3 to 1.8; and (5) near-chondritic Y/Ho ratios of 23.1 to 37.3 (~31 on average). Step 1 for both series display nearly flat REE distribution patterns; step 11 for both series exhibit the largest positive Ce anomalies with $[Ce/Ce^*]_{PAAS}$ ~ 2, the lowest Y/Ho ratios of 15.0 and 13.9, respectively.

For Sample D, the REE concentrations are consistently low in the first ten steps for both series, becoming significantly higher in step 11. The REE distribution patterns are almost uniform for all steps: (1) positive La anomalies with $[La/La^*]_{PAAS}$ ~ 2.3; (2) negative Ce anomalies with $[Ce/Ce^*]_{PAAS}$ ~ 0.6; (3) nearly no Eu anomalies; and (4) super-chondritic Y/Ho ratios of about 52 on average.

3.3. Other diagnostic elements

The masses of other diagnostic elements, including K, Rb, Ti, U, Al, Fe, Mn, and P, in each leachate are also converted into concentration relative to consumed carbonate for each dissolution step. Their variations during the experiment are presented in Fig. 3. It is observed that, the concentrations of K, Rb, Ti, and U are higher in the first few steps, usually steps one to three, showing downward trends. Meanwhile, the contents of Al, Fe, Mn, and P, and also K, Rb, Ti, and U are abnormally high in step 11, being as much as 1 to 4 orders of magnitude greater than in the

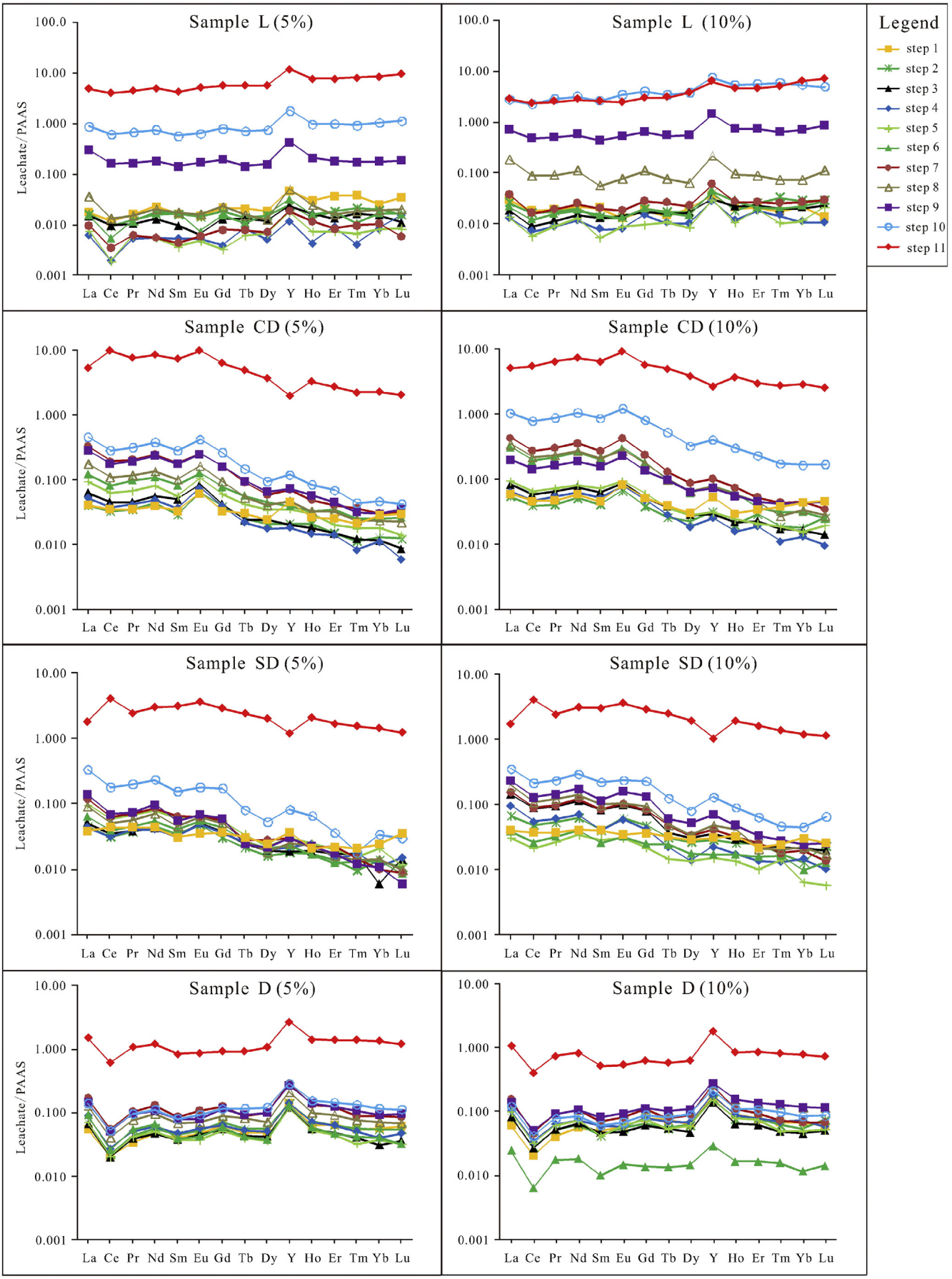

Fig. 2. The PAAS-normalized REE distribution pattern for each leachate.

intermediate steps. Some elements increase from step 9 or 10 in some series, showing upward trends.

4. Discussion

4.1. Preferential dissolution of different carbonate phases

Calcite and dolomite are the two main mineral phases of carbonates. Calcite is a calcium carbonate with minor amount of magnesium, whereas dolomite is a calcium–magnesium carbonate with a Mg/Ca molar ratio around unity. Thus the carbonate mineral phases dissolved in each step can be constrained by the Mg/Ca molar ratio in the corresponding leachate.

Using Sample CD as an example, the Mg/Ca molar ratios are around 0.2 in the leachates for the first three steps and around unity for steps 5–10 (Fig. 1b). This implies that calcite is predominantly dissolved during the first three dissolution steps, and the mineral phase dissolved during steps 5–10 is mainly dolomite. Relative to Sample CD, Sample L contains more calcite which is the predominant phase being dissolved during the first eight steps for its first series and the first seven steps for its second series, and dolomite only becomes the predominant phase during the following two and three steps respectively for the two series. Sample D, which is a very pure dolostone standard material, shows dolomite as the carbonate mineral phase being dissolved during the whole dissolution process. These observations demonstrate in more detail that calcite is preferentially dissolved over dolomite during the dissolution process.

4.2. Effects of carbonate mineral phase on REE distribution pattern

Most Precambrian carbonate rocks contain both calcite and dolomite, and it is demonstrated above that calcite is preferentially dissolved during dissolution using weak acid. It is therefore important to know whether carbonate mineral phases such as calcite and dolomite in the same carbonate rocks share similar REE distribution patterns.

This issue can be addressed by examining the correlation between the Mg/Ca molar ratio and REE distribution pattern of the same leachate. As shown in Fig. 1b and Fig. 2, there is no correlation between shifts in Mg/Ca ratios and changes in REE distribution patterns. For instance, though shifts in Mg/Ca molar ratios for the calcareous dolostone (Sample CD) occur between step 3 and step 5 (Fig. 1b) the similarity in REE distribution patterns of these leachates is striking (Fig. 2). This strongly suggests that the coexisting carbonate phases carry similar REE signals. This conclusion is of crucial importance in extracting REE signals of ambient water mass from carbonate rocks, as most Precambrian carbonate rocks contain both calcite and dolomite, and partial dissolution is the most commonly used method for sample digestion.

4.3. Diagenetic alteration and non-carbonate contamination

Diagenetic alteration (e.g. secondary carbonate phases) and non-carbonate contamination (e.g. clay minerals, Fe–Mn oxyhydroxides, phosphates) are the principal component which must be avoided in the REE study of bulk carbonate rocks. Al, Ti, etc. are typical elements related to terrestrial particulate matter (Bolhar and Van Kranendonk, 2007; Rongemaille et al., 2011); Fe, Mn and P are concentrated in Fe–Mn oxyhydroxides and phosphates respectively. Elements such as K, Rb, and Ti are also very likely to be enriched in secondary carbonate phases or adsorbed on exchangeable sites on mineral surfaces or ion-exchange sites in clay minerals (Montañez et al., 1996; Bailey et al., 2000; Halverson et al., 2007; Li et al., 2013; Liu et al., 2013). Variations of these elements during the stepwise dissolution process can be used to detect the dissolution of non-target materials, and further reveal their effects on the primitive rare earth elements.

4.3.1. Effects on REE concentration

It is observed from Fig. 3 that, the contents of K, Rb, Ti, and U are relatively high in the first few steps and follow a downward trend. This is interpreted as contribution from the dissolution of secondary carbonate phases and perhaps adsorbates on exchangeable sites. However, the REE concentrations in the leachates of these steps are not elevated (Fig. 2), indicating that secondary carbonate phases and adsorbates do not lead to a significant increase in REE concentration.

In contrast, the content of Al, Fe, Mn, and P, and also K, Rb, Ti, and U starts to increase from step 10 or even step 9, and becomes high in step 11 (Fig. 3). This suggests an increasing risk of dissolving non-carbonate minerals in the latter stages of carbonate dissolution, especially when excess acid is added. Correspondingly, the rare earth element contents also exhibit changes in the last few steps, notably step 11 (Fig. 2). This demonstrates that non-carbonate minerals may lead to contamination of REE measurements at the later stage of dissolution.

4.3.2. Effects on REE distribution pattern

In addition to concentration, the REE distribution pattern can be characterized by a number of features, such as a Ce anomaly, Eu anomaly; Y/Ho ratio and the fractionation between LREE and HREE.

4.3.2.1. Ce anomaly. The Ce anomaly is related to the redox state of water. Oxygenated seawater exhibits an obviously negative Ce anomaly, whereas suboxic and anoxic waters have weaker or no Ce anomalies (Wright et al., 1987; Ling et al., 2013). However, the primitive Ce anomalies preserved in carbonate rocks may be contaminated by non-carbonate minerals, such as Fe–Mn oxyhydroxides which are prone to absorb tetravalent cerium and exhibit positive Ce anomalies (Bau et al., 1996; Tachikawa et al., 1999). Therefore, the lowest Ce/Ce^* values are generally considered to be much closer to the true redox state of water. For Sample L, only the intermediate steps, from step 4 to step 7, in the series treated with 5%v/v acetic acid show obviously negative Ce anomalies with $[Ce/Ce^*]_{PAAS}$ ~ 0.5 on average; while other steps, including all steps in the series treated with 10%v/v acetic acid, exhibit no significant Ce anomalies (Fig. 4). It is considered here that Ce anomalies in steps 4–7 for the first series reflect the oxidation state of the seawater, whereas Ce signals from other steps have been affected by non-target materials. For Samples CD and SD, there are no significant Ce anomalies observable in the first ten steps, and they are therefore considered to be an original feature. The positive Ce anomalies in step 11 are most likely to reflect contamination from non-carbonate minerals, such as Fe–Mn oxyhydroxides. For Sample D, all steps exhibit negative Ce anomalies with $[Ce/Ce^*]_{PAAS}$ ~ 0.6 on average. However, the values in step 1 for both series are relatively higher, which should be attributed to the dissolution of secondary carbonate phases and perhaps adsorbates on exchangeable sites.

4.3.2.2. Eu anomaly. In the series of Sample SD, all steps except step 1 exhibit small positive Eu anomalies with $[Eu/Eu^*]_{PAAS}$ ~ 1.5 on average, while step 1 for both series have nearly no Eu anomalies (Fig. 4), further reflecting the influence from secondary carbonates and perhaps adsorbates. For other samples, Eu values are almost uniform during the stepwise dissolution process. The occasionally irregular fluctuations in $[Eu/Eu^*]_{PAAS}$ values are considered to be within experimental error.

4.3.2.3. Y/Ho ratio. Generally, the Y/Ho ratios of typical marine carbonates are strongly super-chondritic (44–74) (Bau et al., 1996), while the ratios of freshwater carbonates are close to chondritic and average upper continental crust (26–28) (Taylor and McLennan, 1985; Kamber et al., 2005). The Y/Ho ratios of marine carbonates would be lowered by non-carbonate contamination, accompanied by elevated contents of Al, Ti, etc. (Webb and Kamber, 2000). In all samples except Sample D, the Y/Ho ratios of step 11 are at their lowest (Fig. 4), which may be attributed to contamination from non-carbonate minerals. In the first

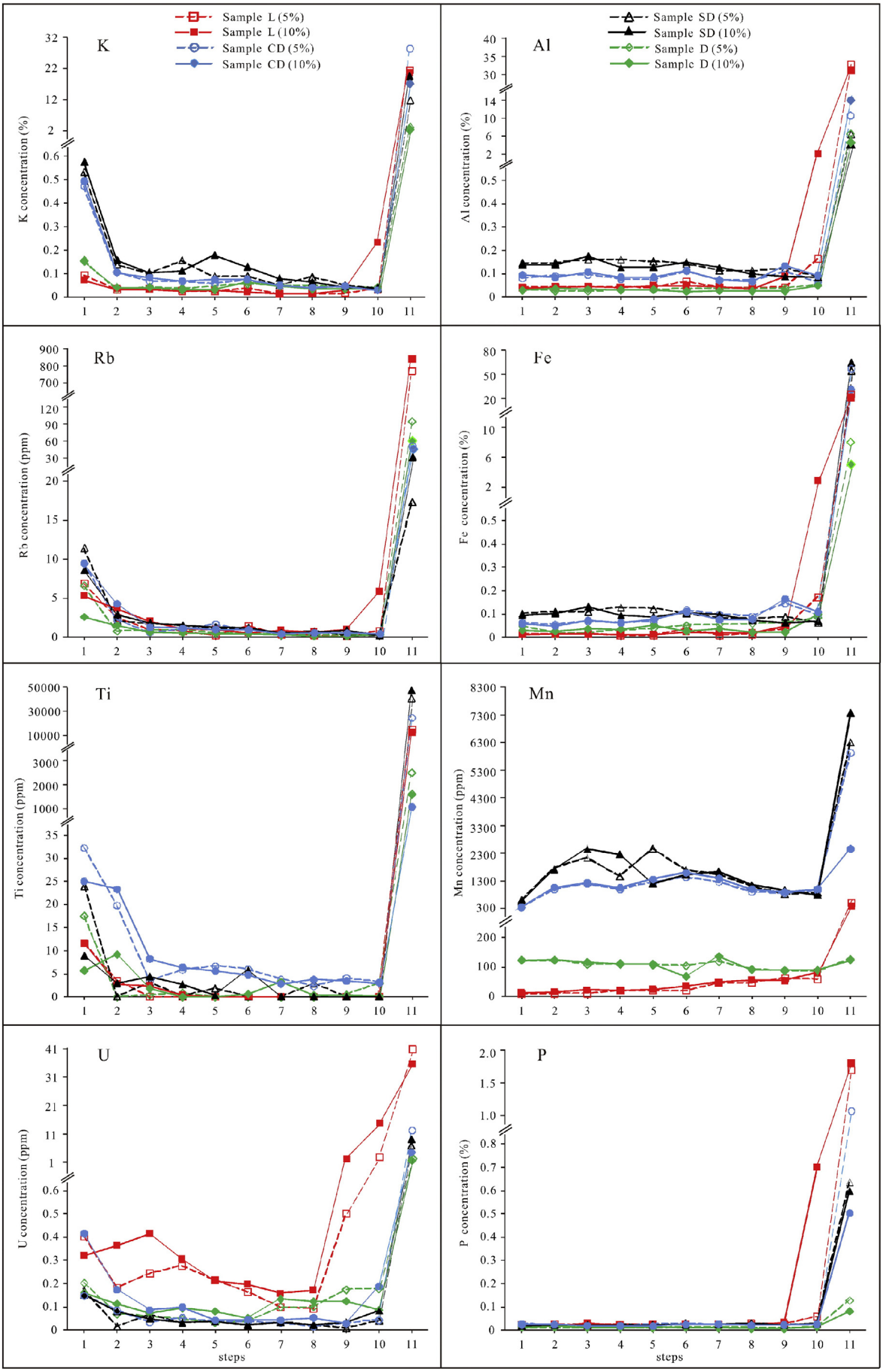

Fig. 3. Variations of other diagnostic element contents in carbonate dissolved during the stepwise dissolution process of samples.

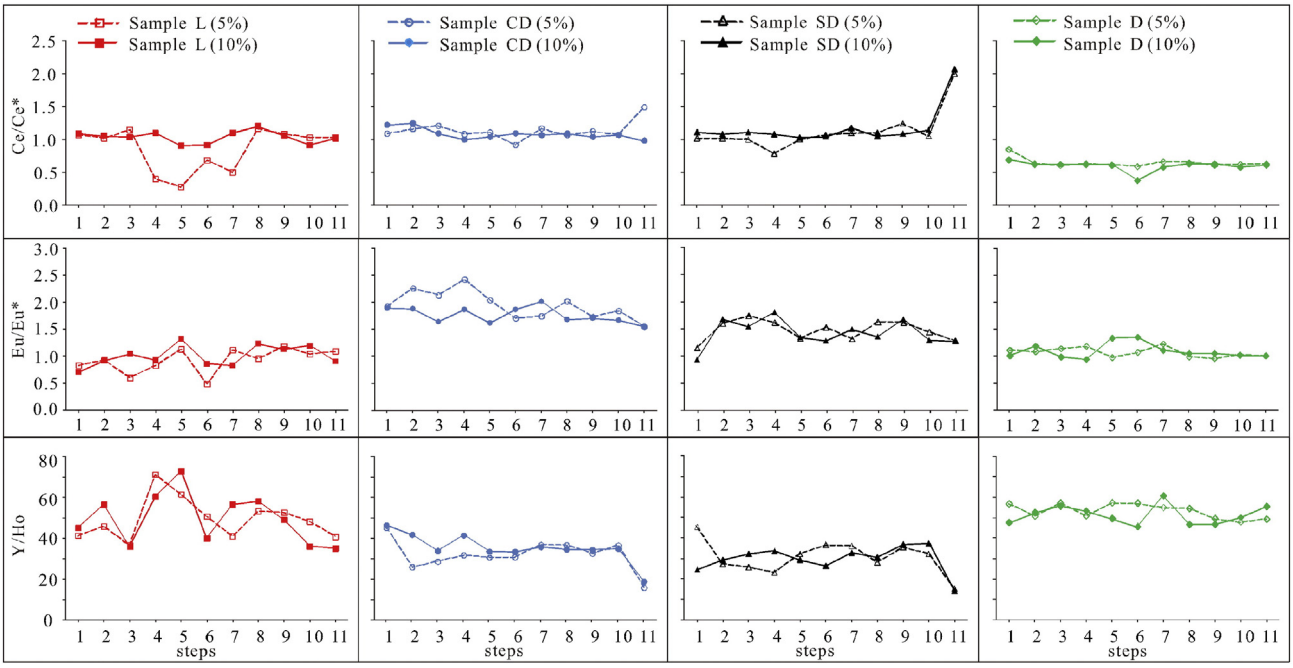

Fig. 4. Variations in Ce anomalies, Eu anomalies and Y/Ho ratios during the stepwise dissolution process of carbonate samples.

ten steps of Sample L, the Y/Ho ratios are generally within the range of typical seawater but show fluctuations, which are regarded as within experimental error due to the low element contents. For Samples CD and SD, the Y/Ho ratios in steps 2–10 are lower than that of typical seawater (Fig. 4). However, these lower Y/Ho ratios are independent of the content of Rb, Al, Ti, etc., and considered to reflect a primitive feature of the parent water. The relatively higher Y/Ho ratios in step 1 (45–46) should be attributed to the dissolution of secondary carbonates and perhaps adsorbates. For Sample D, all the Y/Ho ratios during the stepwise dissolution process are within the range of typical seawater and show small fluctuations, indicating that the influence from non-target materials is minimal.

4.3.2.4. Fractionation between LREE and HREE. In the series of Samples CD and SD, leachates of step 1 exhibit almost flat REE distribution patterns (Fig. 2), indicating little fractionation between LREE and HREE. This differs from the other steps which show LREE enrichment, and may reflect the influence of secondary carbonates and perhaps adsorbates.

In summary, non-carbonate minerals, secondary carbonate phases and adsorbates may affect the primitive REE distribution pattern. For steps which have elevated REE concentrations but similar REE distribution patterns, such as step 10 in the series of Samples CD and SD, step 11 in the series of Sample D (Fig. 2), the REE distribution pattern of contaminant sources may be close to that of the water from which the carbonate rocks precipitated.

4.4. Evaluation of interference from contaminant REE

Averaging of step values of the REE over a range of steps in any series might help to estimate the influence of contaminant REE in a sustained dissolution process, and determine whether it is necessary to discard data, and therefore how much carbonate must be abandoned. Here steps 4–7 are selected as an intermediate selection considering their uniform REE features in one series for all these four samples, then the preceding and following steps are added to this intermediate result (Fig. 5).

For Sample L, in the first series treated with 5%v/v acetic acid, cumulative averages of the REE from step 4 to step 7 (the intermediate from about 35% to 73% of carbonates dissolved) indicate a slight LREE depletion, a positive La anomaly (~1.5), an obviously negative Ce anomaly (~0.5) and a super-chondritic Y/Ho ratio of about 52.2, reflecting an oxidizing marine environment. The cumulative averages of steps 3–7, 2–7, 1–7 and 4–8 show similar REE features with steps 4–7, but weaker negative Ce anomalies, whose $[Ce/Ce^*]_{PAAS}$ values are about 0.7, 0.8, 0.8 and 0.7 respectively, and lower Y/Ho ratios mostly, which are 46.4, 46.3, 44.7 and 52.7 respectively. In contrast, the cumulative averages including steps 9, 10 and 11, such as steps 4–9, 4–10 and 4–11, show obviously increased REE abundances and different REE distribution patterns, exhibiting no Ce anomalies. Accordingly, the initial 30%–40% and final 20%–30% of carbonate is best abandoned if dissolving with 5%v/v acetic acid. In the series treated with 10%v/v acetic acid, even intermediate steps, such as steps 5 and 6 show almost no Ce anomaly with $[Ce/Ce^*]_{PAAS}$ ~ 0.9, indicating possible contamination. Certainly, any kind of REE sampling for this series would not produce a robust result.

Samples CD and SD display analogous REE accumulation cases. Mixing the eleventh leachate into previous selections, such as the cumulative averages of steps 4–11, would greatly increase the REE abundances and change the REE distribution patterns. This is attributed to the significantly high REE concentrations and distinctly different REE distribution patterns in step 11. In this situation excess acid is not advised, and a specific volume of dilute acetic acid needs to be further determined. During the stepwise dissolution processes, leachates from step 2 to step 10 exhibit similar REE distribution patterns (Fig. 2), and thus the cumulative REE distribution patterns among these steps, such as the cumulative averages of steps 4–7, 4–8, 4–9, 4–10, 3–7, 2–7, appear to be uniform. However, the inclusion of the last few steps, notably step 10 (regardless of step 11), with the intermediate part would increase the total REE contents to some extent. The cumulative REE concentrations in the series treated with 10%v/v acetic acid are slightly higher than those in the series treated with 5%v/v acetic acid as a whole. Therefore, 5%v/v acetic acid is more optimal, and at least 10% of total carbonate should remain undissolved for these two samples. Step 1 is notable exhibiting a different REE distribution pattern compared with the intermediate steps though its incorporation with steps 2–7 would in fact not affect the real REE features because of its low concentration. It is noteworthy that, for these two cap carbonate samples both from Doushantuo Formation but different sections, excluding the interferences from secondary carbonates, adsorbates and non-

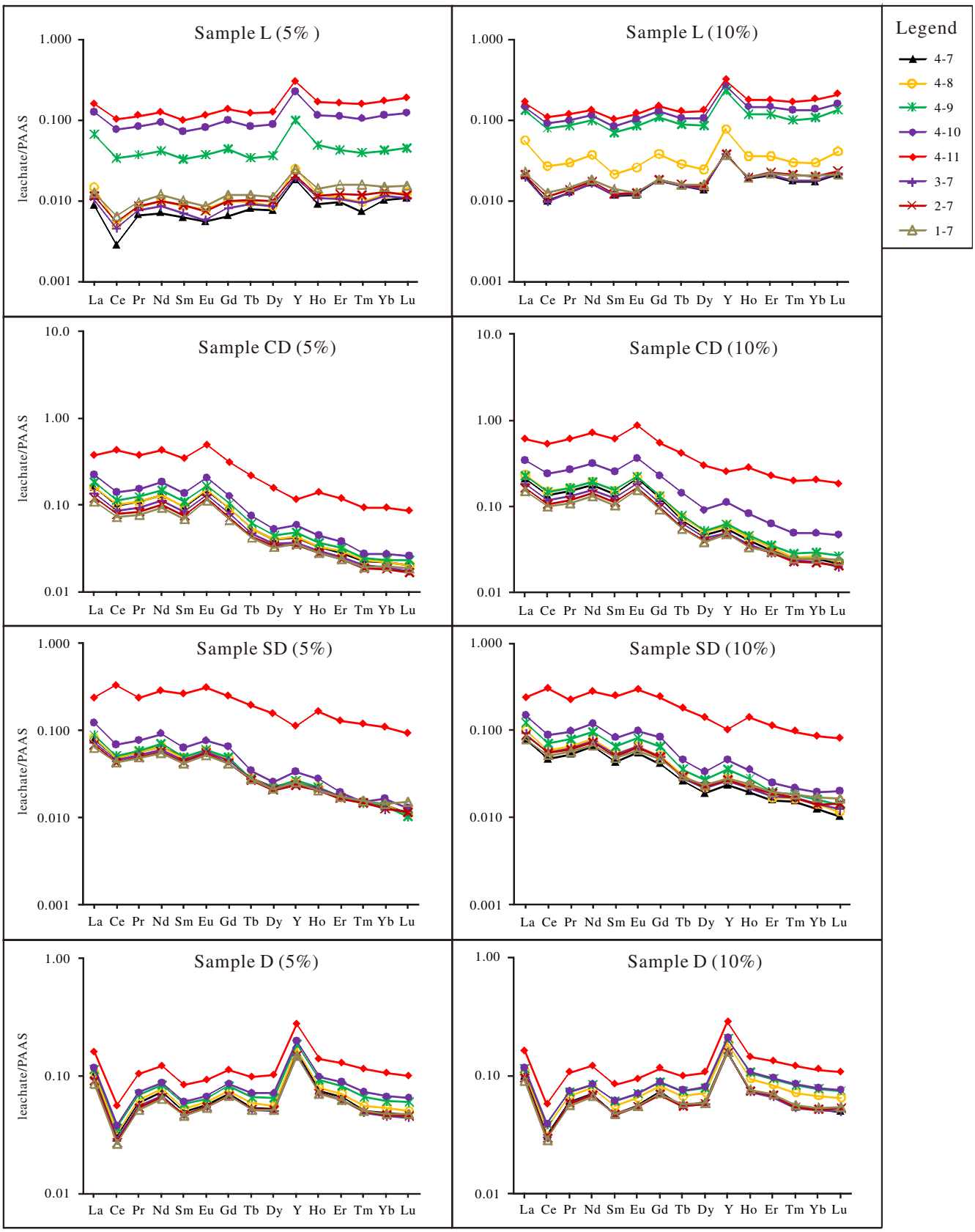

Fig. 5. The cumulative REE distribution patterns. Number 'a–b' at the right side of each legend refers to grouped average of the REE from 'step a' to 'step b'.

carbonate minerals, the REE distribution patterns of the leachates from intermediate steps are distinctly different from those of typical seawater, but similar to those of estuaries (Nothdurft et al., 2004; Lawrence and Kamber, 2006; Wang et al., 2014), providing valuable information regarding the special depositional environment for Marinoan cap carbonates.

For Sample D, all cumulative results, including those mixing the eleventh leachate, show uniform REE distribution patterns. This indicates that the few non-target components in very pure carbonate rocks have little influence on their primitive REE geochemical characteristics, and thus they need little special treatment.

4.5. A refined dissolution method for REE studies of bulk carbonate rocks

Only if diagenetic alteration and non-carbonate contamination are ruled out, can the REE signals of sedimentary carbonates be employed for palaeoenvironmental research. After consideration of data handling in Section 4.4, combined with various diagnostic aspects obtained during the stepwise dissolution process (Fig. 3), a refined dissolution method for REE studies of bulk carbonate rocks is proposed.

The variations of K, Rb, Ti, and U noted during the stepwise dissolution process (Fig. 3) indicate that secondary carbonate phases and adsorbates on exchangeable sites may dissolve preferentially at the beginning of dissolution, equivalent to 30%–40% of total carbonate being dissolved. The study of REE cumulative averages indicates that for some samples, such as those originally showing negative Ce anomalies, the introduction of these non-target materials may affect the apparent primitive REE information. In such cases, an acid preleach (5%v/v acetic acid) dissolving about 30%–40% of carbonate is suggested as a conservative measure. Subsequently 30%–40% of carbonate should be dissolved in 5%v/v acetic acid and separated for REE analysis. 20%–30% of carbonate should remain undissolved to avoid contamination from non-carbonate minerals. REE concentrations in the carbonate components can be obtained by dividing the masses of REE in the chosen leachate fraction by the corresponding weight of ($CaCO_3 + MgCO_3$) which is calculated from the Ca and Mg contents.

5. Conclusions

Our detailed stepwise dissolution experiments demonstrate the dissolution behaviour of various components of bulk carbonate rocks in acid. Their effects on the primitive REE characteristics of the water-column from which the carbonates precipitated are investigated.

Calcite is preferentially dissolved over dolomite during the dissolution process, but neither carbonate mineral phase exerts any specific influence on the measured REE characteristics of carbonate rocks tested. Secondary carbonate phases and adsorbates on exchangeable sites may dissolve preferentially at the beginning of dissolution. This does not appear to lead to any obvious increase in REE concentration, but may affect the detail of the REE distribution pattern, e.g. weakening the negative Ce anomaly, altering the sizes of Eu anomaly and Y/Ho ratio, modifying the degree of the fractionation between LREE and HREE. Non-carbonate minerals such as terrestrial particulate matter, Fe–Mn oxyhydroxides and phosphates are most likely to be dissolved towards the end of dissolution, especially when excess acid is added. This may act to increase the REE concentration and change the resultant REE distribution pattern significantly. In contrast, leachates from intermediate dissolution steps show reduced apparent contamination. Relative to leachates using 10%v/v acetic acid, those extracted with 5%v/v acetic acid return REE information which appears to better reflect that of the water-column from which the carbonates precipitated.

A refined dissolution method for rare earth element studies of bulk carbonate rocks is proposed. An acid preleach (5%v/v acetic acid) dissolving about 30%–40% of total carbonate is recommended, followed by dissolution of 30%–40% of total carbonate in 5%v/v acetic acid to be separated for REE analysis. 20%–30% of total carbonate should remain undissolved in order to avoid contamination from non-carbonate minerals. In addition, REE concentrations in carbonate components can be obtained by dividing the masses of REE in the selected leachate by the corresponding weight of ($CaCO_3 + MgCO_3$) which is calculated from the total Ca and Mg contents.

Acknowledgements

This work was supported by the MLR Public Benefit Research Foundation (201411044) and the National Natural Science Foundation of China (41430104, 41303003). Dr. Hongfei Ling and other two anonymous official reviewers are thanked for their helpful comments. Dr. Nick Belshaw is thanked for polishing the English language, and Dr. David Hilton is thanked for his professional handling of the paper. We thank Zhao-Fu Gao and Fei-Fei Zhang for assistance with field work, and thank Suo-Han Tang, Yue-Ling Guo, Jin Li, Jian Sun, Ai-Guo Dong, Chen-Xu Pan, and Jian-Xiong Ma for their meticulous guidance during the chemical experiments at CAGS. Qian Liu, Li-Wen Qiu and Fei-Peng Xu are also thanked for their help with the ICP-MS and ICP-AES determinations at Nanjing University.

Appendix A. Supplementary data

Supplementary data to this article can be found online at http://dx.doi.org/10.1016/j.chemgeo.2015.07.027.

References

Bailey, T.R., McArthur, J.M., Prince, H., Thirlwall, M.F., 2000. Dissolution methods for strontium isotope stratigraphy: whole rock analysis. Chem. Geol. 167, 313–319.
Banner, J.L., Hanson, G.N., 1990. Calculation of simultaneous isotopic and trace element variations during water–rock interaction with applications to carbonate diagenesis. Geochim. Cosmochim. Acta 54, 3123–3137.
Banner, J.L., Hanson, G.N., Meyers, W.J., 1988. Rare earth element and Nd isotopic variations in regionally extensive dolomites from the Burlington–Keokuk Formation (Mississippian): implication for REE mobility during carbonate diagenesis. J. Sediment. Petrol. 58, 415–432.
Bau, M., Koschinsky, A., Dulski, P., Hein, J.R., 1996. Comparison of the partitioning behaviours of yttrium, rare earth elements, and titanium between hydrogenetic marine ferromanganese crusts and seawater. Geochim. Cosmochim. Acta 60, 1709–1725.
Birgel, D., Feng, D., Roberts, H.H., Peckmann, J., 2011. Changing redox conditions at cold seeps as revealed by authigenic carbonates from Alaminos Canyon, northern Gulf of Mexico. Chem. Geol. 285, 82–96.
Bolhar, R., Van Kranendonk, M.J., 2007. A non-marine depositional setting for the northern Fortescue Group, Pilbara Craton, inferred from trace element geochemistry of stromatolitic carbonates. Precambrian Res. 155, 229–250.
Bolhar, R., Kamber, B.S., Moorbath, S., Fedo, C.M., Whitehouse, M.J., 2004. Characterisation of early Archaean chemical sediments by trace element signatures. Earth Planet. Sci. Lett. 222, 43–60.
Cantrell, K.J., Byrne, R.H., 1987. Rare earth element complexation by carbonate and oxalate ions. Geochim. Cosmochim. Acta 51, 597–605.
Danielson, A., Möller, P., Dulski, P., 1992. The europium anomalies in banded iron formations and the thermal history of the oceanic crust. Chem. Geol. 97, 89–100.
Delpomdor, F., Blanpied, C., Virgone, A., Préat, A., 2013. Paleoenvironments in Meso-Neoproterozoic carbonates of the Mbuji–Mayi Supergroup (Democratic Republic of Congo) — microfacies analysis combined with C–O–Sr isotopes, major-trace elements and REE + Y distributions. J. Afr. Earth Sci. 88, 72–100.
Derry, L.A., Jacobsen, S.B., 1990. The chemical evolution of Precambrian seawater: evidence from REEs in banded iron formations. Geochim. Cosmochim. Acta 54, 2965–2977.
Elderfield, H., 1986. Strontium isotope stratigraphy. Palaeogeogr. Palaeoclimatol. Palaeoecol. 57, 71–90.
Elderfield, H., Sholkovitz, E.R., 1987. Rare earth elements in the pore waters of reducing nearshore sediments. Earth Planet. Sci. Lett. 82, 280–288.
Elderfield, H., Hawkesworth, C.J., Greaves, M.J., 1981. Rare earth element geochemistry of oceanic ferromanganese nodules and associated sediments. Geochim. Cosmochim. Acta 45, 513–528.
Elderfield, H., Upstill-Goddard, R., Sholkovitz, E.R., 1990. The rare earth elements in rivers, estuaries and coastal seas and their significance to the composition of ocean waters. Geochim. Cosmochim. Acta 54, 971–991.
Frimmel, H.E., 2009. Trace element distribution in Neoproterozoic carbonates as palaeoenvironmental indicator. Chem. Geol. 258, 338–353.
García, M.G., Lecomte, K.L., Pasquini, A.I., Formica, S.M., Depetris, P.J., 2007. Sources of dissolved REE in mountainous streams draining granitic rocks, Sierras Pampeanas (Córdoba, Argentina). Geochim. Cosmochim. Acta 71, 5355–5368.
Ge, L., Jiang, S.Y., Swennen, R., Yang, T., Yang, J.H., Wu, N.Y., Liu, J., Chen, D.H., 2010. Chemical environment of cold seep carbonate formation on the northern continental slope of South China Sea: evidence from trace and rare earth element geochemistry. Mar. Chem. 277, 21–30.
Halverson, G.P., Dudás, F.Ö., Maloof, A.C., Bowring, S.A., 2007. Evolution of the $^{87}Sr/^{86}Sr$ composition of Neoproterozoic seawater. Palaeogeogr. Palaeoclimatol. Palaeoecol. 256, 103–129.
Kamber, B.S., Greig, A., Collerson, K.D., 2005. A new estimate for the composition of weathered young upper continental crust from alluvial sediments, Queensland, Australia. Geochim. Cosmochim. Acta 69, 1041–1058.

Lawrence, M.G., Kamber, B.S., 2006. The behavior of the rare earth elements during estuarine mixing-revisited. Mar. Chem. 100, 147–161.
Lawrence, M.G., Greig, A., Collerson, K.D., Kamber, B.S., 2006. Rare earth element and yttrium variability in South East Queensland waterways. Aquat. Geochem. 12, 39–72.
Lee, J.H., Byrne, R.H., 1993. Complexation of trivalent rare earth elements (Ce, Eu, Gd, Tb, Yb) by carbonate ions. Geochim. Cosmochim. Acta 57, 295–302.
Li, D., Shields-Zhou, G.A., Ling, H.F., Thirlwall, M., 2011. Dissolution methods for strontium isotope stratigraphy: guidelines for the use of bulk carbonate and phosphorite rocks. Chem. Geol. 290, 133–144.
Li, D., Ling, H.F., Shields-Zhou, G.A., Chen, X., Cremonese, L., Och, L., Thirlwall, M., Manning, C.J., 2013. Carbon and strontium isotope evolution of seawater across the Ediacaran–Cambrian transition: evidence from the Xiaotan section, NE Yunnan, South China. Precambrian Res. 225, 128–147.
Lin, Z.J., Wang, Q.X., Feng, D., Liu, Q., Chen, D.F., 2011. Post-depositional origin of highly ^{13}C-delepted carbonate in the Doushantuo cap dolostone in South China: insights from petrography and stable carbon isotopes. Sediment. Geol. 242, 71–79.
Ling, H.F., Chen, X., Li, D., Wang, D., Shields-Zhou, G.A., Zhu, M.Y., 2013. Cerium anomaly variations in Ediacaran-earliest Cambrian carbonates from the Yangtze Gorges area, South China: implications for oxygenation of coeval shallow seawater. Precambrian Res. 225, 110–127.
Liu, C., Wang, Z.R., Raub, T.D., 2013. Geochemical constraints on the origin of Marinoan cap dolostones from Nuccaleena Formation, South Australia. Chem. Geol. 351, 95–104.
Loope, G.R., Kump, L.R., Arthur, M.A., 2013. Shallow water redox conditions from the Permian-Triassic boundary microbialite: the rare earth element and iodine geochemistry of carbonates from Turkey and South China. Chem. Geol. 351, 195–208.
Montañez, I.P., Banner, J.L., Osleger, D.A., Borg, L.E., Bosserman, P.J., 1996. Integrated Sr isotope variations and sea-level history of Middle to Upper Cambrian platform carbonates: implications for the evolution of Cambrian seawater ^{87}Sr/^{86}Sr. Geology 24, 917–920.
Nothdurft, L.D., Webb, G.E., Kamber, B.S., 2004. Rare earth element geochemistry of Late Devonian reefal carbonates, Canning Basin, Western Australia: confirmation of a seawater REE proxy in ancient limestones. Geochim. Cosmochim. Acta 68, 263–283.
Nozaki, Y., Zhang, J., Amakawa, H., 1997. The fractionation between Y and Ho in the marine environment. Earth Planet. Sci. Lett. 148, 329–340.
Pourret, O., Davranche, M., Gruau, G., Dia, A., 2007. Competition between humic acid and carbonates for rare earth elements complexation. J. Colloid Interface Sci. 305, 25–31.
Rongemaille, E., Bayon, G., Pierre, C., Bollinger, C., Chu, N.C., Fouquet, Y., Riboulot, V., Voisset, M., 2011. Rare earth elements in cold seep carbonates from the Niger delta. Chem. Geol. 286, 196–206.
Shields, G., Stille, P., 2001. Diagenetic constraints on the use of cerium anomalies as palaeoseawater redox proxies: an isotopic and REE study of Cambrian phosphorites. Chem. Geol. 175, 29–48.
Shields, G.A., Webb, G.E., 2004. Has the REE composition of seawater changed over geological time? Chem. Geol. 204, 103–107.
Sholkovitz, E.R., Piepgras, D.J., Jacobsen, S.B., 1989. The pore water chemistry of rare earth elements in Buzzards Bay sediments. Geochim. Cosmochim. Acta 53, 2847–2856.
Sholkovitz, E.R., Elderfield, H., Szymczak, R., Casey, K., 1999. Island weathering: river sources of rare earth elements to the Western Pacific Ocean. Mar. Chem. 68, 39–57.
Slack, J.F., Grenne, T., Bekker, A., Rouxel, O.J., Lindberg, P.A., 2007. Suboxic deep seawater in the late Paleoproterozoic: evidence from hematitic chert and iron formation related to seafloor-hydrothermal sulfide deposits, central Arizona, USA. Earth Planet. Sci. Lett. 255, 243–256.
Tachikawa, K., Jeandel, C., Vangriesheim, A., Dupré, B., 1999. Distribution of rare earth elements and neodymium isotopes in suspended particles of the tropical Atlantic Ocean (EUMELI site). Deep-Sea Res. I Oceanogr. Res. Pap. 46, 733–755.
Taylor, S.R., McLennan, S.M., 1985. The Continental Crust: Its Composition and Evolution. Blackwell Scientific Publications, Oxford, UK.
Wang, Q.X., Lin, Z.J., Chen, D.F., 2014. Geochemical constraints on the origin of Doushantuo cap carbonates in the Yantze Gorges area, South China. Sediment. Geol. 304, 59–70.
Webb, G.E., Kamber, B.S., 2000. Rare earth elements in Holocene reefal microbialites: a new shallow seawater proxy. Geochim. Cosmochim. Acta 64, 1557–1565.
Wheat, C.G., Mottl, M.J., Rudnicki, M., 2002. Trace element and REE composition of a low-temperature ridge-flank hydrothermal spring. Geochim. Cosmochim. Acta 66, 3693–3705.
Wright, J., Schrader, H., Holser, W.T., 1987. Paleoredox variations in ancient oceans recorded by rare earth elements in fossil apatite. Geochim. Cosmochim. Acta 51, 631–644.
Zhang, J., Nozaki, Y., 1996. Rare earth elements and yttrium in seawater: ICP-MS determinations in the East Caroline, Coral Sea, and South Fiji basins of the western South Pacific Ocean. Geochim. Cosmochim. Acta 60, 4631–4644.
Zhao, Y.Y., Zheng, Y.F., Chen, F.K., 2009. Trace element and strontium isotope constraints on sedimentary environment of Ediacaran carbonates in southern Anhui, South China. Chem. Geol. 265, 345–362.